Vehicle System Dynamics
Vol. 50, No. 8, August 2012, 1209–1224

Taylor & Francis
Taylor & Francis Group

Lateral dynamics of a bicycle with a passive rider model: stability and controllability

A.L. Schwab[a]*, J.P. Meijaard[b] and J.D.G. Kooijman[a]

[a]*Laboratory for Engineering Mechanics, Delft University of Technology, Mekelweg 2, NL 2628 CD Delft, The Netherlands;* [b]*Mechanical Automation and Mechatronics, Faculty of Engineering Technology, University of Twente, Enschede, The Netherlands*

(*Received 18 May 2011; final version received 23 July 2011*)

This paper addresses the influence of a passive rider on the lateral dynamics of a bicycle model and the controllability of the bicycle by steer or upper body sideway lean control. In the uncontrolled model proposed by Whipple in 1899, the rider is assumed to be rigidly connected to the rear frame of the bicycle and there are no hands on the handlebar. Contrarily, in normal bicycling the arms of a rider are connected to the handlebar and both steering and upper body rotations can be used for control. From observations, two distinct rider postures can be identified. In the first posture, the upper body leans forward with the arms stretched to the handlebar and the upper body twists while steering. In the second rider posture, the upper body is upright and stays fixed with respect to the rear frame and the arms, hinged at the shoulders and the elbows, exert the control force on the handlebar. Models can be made where neither posture adds any degrees of freedom to the original bicycle model. For both postures, the open loop, or uncontrolled, dynamics of the bicycle–rider system is investigated and compared with the dynamics of the rigid-rider model by examining the eigenvalues and eigenmotions in the forward speed range 0–10 m/s. The addition of the passive rider can dramatically change the eigenvalues and their structure. The controllability of the bicycles with passive rider models is investigated with either steer torque or upper body lean torque as a control input. Although some forward speeds exist for which the bicycle is uncontrollable, these are either considered stable modes or are at very low speeds. From a practical point of view, the bicycle is fully controllable either by steer torque or by upper body lean, where steer torque control seems much easier than upper body lean.

Keywords: bicycle dynamics; non-holonomic systems; multibody dynamics; human control; modal controllability

1. Introduction

The bicycle is an intriguing machine as it is laterally unstable at low speeds and stable, or easy to stabilise, at high speeds. During the last decade a revival in the research on dynamics and control of bicycles has taken place [1–3]. Most studies use the so-called Whipple model [4] of a bicycle. In this model, a hands-free rigid rider is fixed to the rear frame. However, from experience it is known that some form of control is required to stabilise the bicycle and follow a path. This control is either applied by steering or by performing some set of upper body

*Corresponding author. Email: a.l.schwab@tudelft.nl

ISSN 0042-3114 print/ISSN 1744-5159 online

http://dx.doi.org/10.1080/00423114.2011.610898
http://www.tandfonline.com

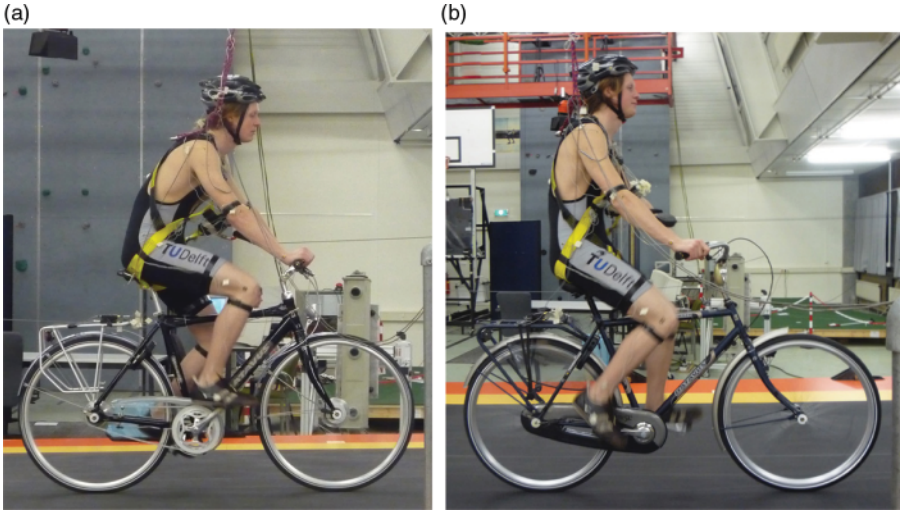

Figure 1. Bicycling on a treadmill, two distinct postures: (a) Rider A on the hybrid bicycle with body leaned forward and stretched arms and (b) Rider A on the city bicycle with an upright body and flexed arms.

motions. The precise control used by the rider is currently under study [5,6]. Here, we focus on two subjects: (i) the contribution of passive body motions to the uncontrolled dynamics of a bicycle, and (ii) the controllability of these extended models with either steering or upper body lean as a control input.

From observations [5,6], two distinct rider postures can be identified. In the first posture, the upper body leans forward with stretched arms on the handlebar, see Figure 1(a). For steering, the upper body needs to twist. In the second rider posture, the upper body stays upright and fixed with respect to the rear frame and the arms, hinging at the shoulders and the elbows, are connected to the handlebar, see Figure 1(b). For both postures, models can be made with the same number of degrees of freedom as the original Whipple bicycle model. In other words, both rider models just add a mechanism to the original system without any additional degrees of freedom. In order to describe the control by applying a lean torque from the lower body to the upper body, both posture models are extended with an extra degree of freedom to describe the upper body lean.

Only a few people have investigated the controllability of a bicycle. Nagai [7] used a simple bicycle model in which only the rear frame and rider have mass, the trail is zero and the steer angle and upper body sideway lean angle are kinematic control inputs. He finds one non-zero forward speed and one condition on the mass distribution which result in uncontrollability for the system. Seffen *et al.* [8] investigate controllability for a bicycle model similar to the model derived by Sharp [9] with steer torque as the control input. They introduce an index, based on [10], which should indicate the difficulty of riding. The index is based on the ratio of the largest and smallest singular values of the controllability matrix. Neither work addresses whether the uncontrollable mode is stable or unstable, although Seffen *et al*. [8] mention stabilisability. It could well be that the uncontrollable or nearly uncontrollable mode is a stable mode of the system that is inessential for the desired output and therefore of no concern to the rider. This paper tries to resolve that problem by determining the forward speed at which the bicycle is uncontrollable and then identifying whether this corresponds to a stable or unstable mode. This approach results in discrete speeds for which the system is uncontrollable. To investigate the controllability by a continuous measure, the concept of modal controllability, as introduced by Hamdan and Nayfeh [11], is applied.

The paper is organised as follows. First the original bicycle model is presented. Next the extension of this model with a twisting upper body or flexed arms is presented and the stability of the lateral motions is compared with that of a rigid rider model in a forward speed range 0–10 m/s. Then the models are extended with a degree of freedom for the upper body sideway lean and the controllability is investigated for the two cases in which either the steer torque or the upper body lean torque is a control input. The paper ends with some conclusions. The appendix summarises the data for the bicycle models.

2. Bicycle model

The basic bicycle model used is the so-called Whipple model [4], which recently has been benchmarked [2]. The model, see Figure 2, consists of four rigid bodies connected by revolute joints. The contact between the knife-edged wheels and the flat level surface is modelled by holonomic constraints in the normal direction, prescribing the wheels to touch the surface, and by non-holonomic constraints in the longitudinal and lateral directions, prescribing zero longitudinal and lateral slips. In this original model, it is assumed that the rider is rigidly attached to the rear frame and has no hands on the handlebar. The resulting non-holonomic mechanical model has three velocity degrees of freedom: forward speed v, lean rate $\dot{\phi}$ and steering rate $\dot{\delta}$.

For the stability analysis of the lateral motions, we consider the linearised equations of motion for small perturbations about the upright steady forward motion. These linearised equations of motion are fully described in [2]. They are expressed in terms of small changes in the lateral degrees of freedom (the rear frame roll angle, ϕ, and the steering angle, δ) from the upright straight-ahead configuration $(\phi, \delta) = (0, 0)$, at a forward speed v, and have the form

$$\mathbf{M}\ddot{\mathbf{q}} + v\mathbf{C}_1\dot{\mathbf{q}} + [g\mathbf{K}_0 + v^2\mathbf{K}_2]\mathbf{q} = \mathbf{f}, \tag{1}$$

where the time-varying variables are $\mathbf{q} = [\phi, \delta]^{\mathrm{T}}$ and the lean and steering torques are $\mathbf{f} = [T_\phi, T_\delta]^{\mathrm{T}}$. The coefficients in this equation are: a constant symmetric mass matrix, $\mathbf{M}$, a damping-like (there is no real damping) matrix, $v\mathbf{C}_1$, which is linear in the forward speed v, and a stiffness matrix which is the sum of a constant symmetric part, $g\mathbf{K}_0$, and a part, $v^2\mathbf{K}_2$, which is quadratic in the forward speed. The forces on the right-hand side, $\mathbf{f}$, are the applied forces which are energetically dual to the degrees of freedom $\mathbf{q}$. In the upright straight-ahead

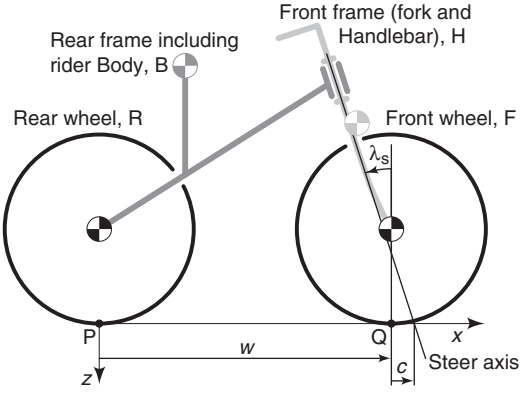

Figure 2. The bicycle model: four rigid bodies (rear wheel R, rear frame B, front handlebar assembly H and front wheel F) connected by three revolute joints (rear hub, steering axis and front hub), together with the coordinate system.

configuration, the linearised equation of motion for the forward motion is decoupled from the linearised equations of motion of the lateral motions and simply reads $\dot{v} = 0$.

Besides the equations of motion, kinematic differential equations for the configuration variables that are not degrees of freedom have to be added to complete the description. For the forward motion, the equations for the rotation angles of the wheels are $\dot{\theta}_R = -v/r_R$, $\dot{\theta}_F = -v/r_F$, where θ_R and θ_F are the rotation angles of the rear and front wheel and r_R and r_F are the corresponding wheel radii. For the lateral motion, the equations for the yaw (heading) angle, ψ, and the lateral displacement of the rear wheel contact point, y_P, are $\dot{\psi} = (v\delta + c\dot{\delta})\cos\lambda_s/w$ and $\dot{y}_P = v\psi$. For the case of the bicycle, these equations can be considered as a system in series with the system defined by the equations of motion (1) with $\mathbf{q}$ and $\dot{\mathbf{q}}$ as inputs and the configuration variables as outputs. The stability and controllability of the two systems can therefore be studied separately.

The entries in the constant coefficient matrices $\mathbf{M}$, $\mathbf{C}_1$, $\mathbf{K}_0$ and $\mathbf{K}_2$ can be calculated from a non-minimal set of 25 bicycle parameters as described in [2]. A procedure for measuring these parameters for a real bicycle is described in [12], whereas measured values for the bicycles used in this study are listed in Table A2 of the appendix. Then, with the coefficient matrices the characteristic equation,

$$\det(\mathbf{M}\lambda^2 + v\mathbf{C}_1\lambda + g\mathbf{K}_0 + v^2\mathbf{K}_2) = 0, \tag{2}$$

can be formed and the eigenvalues, λ, can be calculated. In principle, there are up to four eigenmodes, where oscillatory eigenmodes come in pairs. Two are significant and are traditionally called the *capsize* mode and the *weave* mode, see Figure 3(a). The capsize mode corresponds to a real eigenvalue with an eigenvector dominated by lean: when unstable, the bicycle follows a spiralling path with increasing curvature until it falls. The weave mode is an oscillatory motion in which the bicycle sways about the heading direction. The third remaining eigenmode is the overall stable *castering* mode, like in a trailing caster wheel, which corresponds to a large negative real eigenvalue with an eigenvector dominated by steering. The eigenvalues corresponding to the kinematic differential equations are all zero and correspond to changes in the rotation angles of the wheels, a constant yaw angle and a linearly increasing lateral displacement.

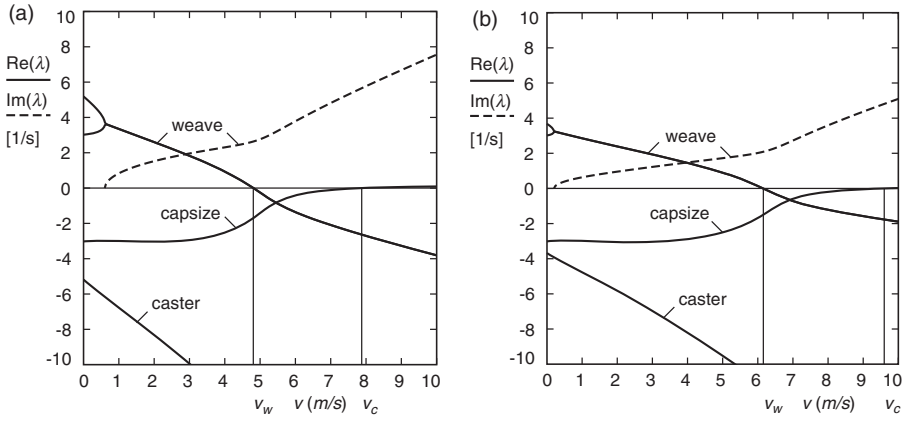

Figure 3. Eigenvalues for the lateral motions of a bicycle–rider combination in a forward speed range of $0\,\mathrm{m/s} < v < 10\,\mathrm{m/s}$, (a) with a completely rigid rider and hands-free and (b) with a rider with stretched arms, hands on the handlebar and a yawing upper body according to the model from Figure 4(a). Note that the bicycle is passively self-stable between the weave speed v_w and the capsize speed v_c.

At near-zero speeds, typically $0\,\mathrm{m/s} < v < 0.5\,\mathrm{m/s}$, there are two pairs of real eigenvalues. Each pair consists of a positive and a negative eigenvalue and corresponds to an inverted-pendulum-like falling of the bicycle. The positive root in each pair corresponds to falling, whereas the negative root corresponds to a righting motion. For $v = 0$, these two are related by a time reversal of the motion. When speed is increased, two real eigenvalues coalesce and then split to form a complex conjugate pair; this is where the oscillatory weave motion emerges. At first, this motion is unstable, but at $v = v_{\mathrm{w}} \approx 4.8\,\mathrm{m/s}$, the weave speed, these eigenvalues cross the imaginary axis at a Hopf bifurcation and this mode becomes stable. At a higher speed, the capsize eigenvalue crosses the origin at a pitchfork bifurcation at $v = v_{\mathrm{c}} \approx 7.9\,\mathrm{m/s}$, the capsize speed, and the bicycle becomes mildly unstable. The speed range for which the uncontrolled bicycle shows asymptotically stable behaviour, with all eigenvalues having negative real parts, is $v_{\mathrm{w}} < v < v_{\mathrm{c}}$.

3. Passive rider models

The original Whipple model is extended with a passive rider without adding any degrees of freedom. From observations of riding on a large treadmill ($3 \times 5\,\mathrm{m}^2$) [5,6], two distinct postures emerged which are both modelled. In the first posture model the upper body is leaned forward and the arms are stretched and connected to the handlebar whereas the upper body is allowed to twist, see Figure 4(a). The second posture model has a rigid upper body connected to the rear frame and hinged arms at the shoulder and elbow connected to the handlebar, see Figure 4(b). Neither model adds any degree of freedom to the original Whipple model. This means that the number and structure of the linearised equations of motion (1) stay the same and only the entries in the matrices change.

For the modelling of the geometry and mass properties of the rider, the method as described by Moore *et al.* [13] is used. Here the human rider is divided into a number of simple geometric objects, namely cylinders, blocks and a sphere of constant density (see Figure A1(a) in the appendix). Then with the proper dimensions and the estimates of the masses of the individual body parts and the necessary skeleton points describing the posture, the mechanical model can be made. For Rider A used in this study, these anthropomorphic data can be found in Table A3 of the appendix, whereas the procedure for calculating the necessary skeleton points is presented in Table A4 of the appendix.

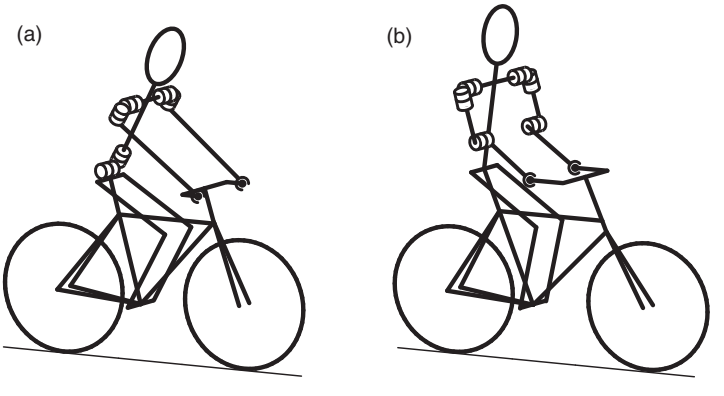

Figure 4. Two distinct bicycle models which include a passive rider: (a) rider with forward leaned body and stretched arms and (b) rider with upright body and flexed arms.

The geometric and mass properties of the two bicycles used in this study were obtained by the procedure described in [12] and the results are presented in Tables A1 and A2 of the appendix.

The complete model of the bicycle with a passive rider was analysed with the multibody dynamics software package SPACAR [14]. This package can handle systems of rigid and flexible bodies connected by various joints in both open and closed kinematic loops, where parts may have rolling contact [15,16]. The package generates numerically, and solves, full non-linear dynamics equations using minimal coordinates (constraints are eliminated). It can also be used to find the numeric coefficients for the linearised equations of motion based on a semi-analytic linearisation of the non-linear equations. This technique has been used here to generate the constant coefficient matrices $\mathbf{M}$, $\mathbf{C}_1$, $\mathbf{K}_0$ and $\mathbf{K}_2$ from the linearised equations of motion (1), which serve as a basis for generating the eigenvalues of the lateral motions in the desired forward speed range.

3.1. *Forward leaned passive rider*

In the model for leaned forward posture, the arms are stretched and the upper and lower arms are modelled as one rigid body each, connected by universal joints to the torso and by ball joints to the handlebar (see Figure 4(a)). The torso is allowed to twist and pitch. Note that in a first-order approximation, the pitching motion is zero, which follows directly from symmetry arguments. The legs are rigidly attached to the rear frame. The linearised equations of motion are derived as described above and the eigenvalues and eigenmotions of the lateral motions are calculated in a forward speed range 0–10 m/s. These eigenvalues are shown in Figure 3(b). For comparison, the eigenvalues of a Whipple-like rigid rider model are shown in Figure 3(a). In the rigid rider model we assume the same forward leaned posture but now with no hands on the handlebar and the complete rider rigidly attached to the rear frame.

Compared with the rigid rider solutions, there are some small changes in the eigenvalues, but the overall structure is the same. Most noticeable are that the stable speed range goes up and that the frequency of the weave motion goes down. These changes can be explained from two major contributing factors. The first is that the attached passive mechanism of arms and twisting upper body adds a mass moment of inertia to the steering assembly. This increases the diagonal mass term $M_{\delta\delta}$ of the mass matrix for the steering degree of freedom from 0.28 to 0.72 kg m^2. The off-diagonal terms increase slightly (10%). The added mass increases the weave speed and decreases the weave frequencies over the considered speed range. The second factor is the added stiffness to the steering assembly due to the compressive forces exerted by the hands on the handlebar. This affects several entries in the matrices of the linearised equations; the most noticeable are the changes in the symmetric static stiffness matrix $g\mathbf{K}_0$. The diagonal term for the steering stiffness, $gK_{0\delta\delta}$, decreases from -6.9 to -9.7 N m/rad and the off-diagonal terms decrease by 10%. The effects on the eigenvalues are an increased weave and capsize speed and an overall decrease of weave frequencies, whereas the structure of the eigenvalues with respect to the forward speed remains about the same. It should also be noted that the more the direction of the stretched arms is parallel to the steer axis, the less the change in the dynamics compared with the rigid rider model is.

3.2. *Upright passive rider*

In the upright posture, the torso and the legs are rigidly connected to the rear frame. The upper arms are connected to the torso by universal joints and the lower arms are connected to the upper arms by single hinges at the elbows and by ball joints at the handlebar (see Figure 4(b)).

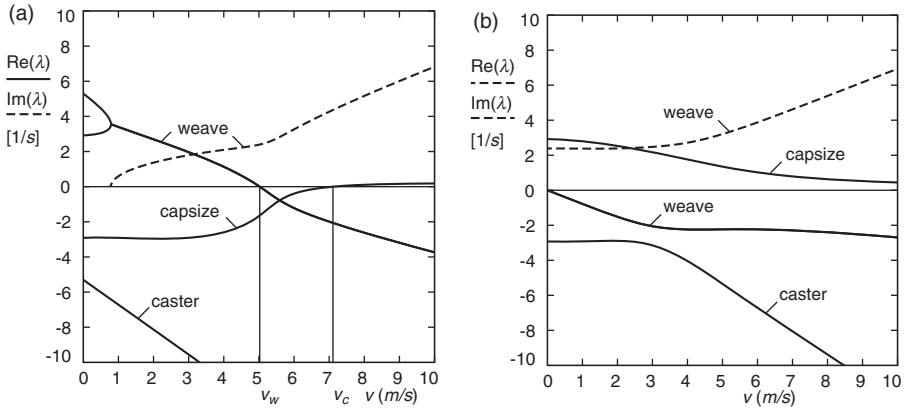

Figure 5. Eigenvalues for the lateral motions of a bicycle–rider combination (a) with a fully rigid rider and hands-free and (b) with a rider with rigid upper body and flexed arms and hands on the handlebar according to the model from Figure 4(b).

The linearised equations of motion are derived as described above and the eigenvalues of the lateral motions are computed. These eigenvalues are shown in Figure 5(b). For comparison, the eigenvalues of a Whipple-like rigid rider model are shown in Figure 5(a). In the rigid rider model, we assume the same upright posture, but now with no hands on the handlebar and the complete rider rigidly attached to the rear frame.

Compared with the rigid rider solutions, there are dramatic changes in the eigenvalues and their structure. The stable forward speed range has disappeared completely, because the weave speed has decreased to zero and the capsize motion is always unstable. Note that the weave motion is now always stable but gets washed out by the unstable capsize. This dramatic change can be explained as follows. By adding the hinged arms to the handlebar, a stable pendulum-type of oscillator has been added to the steer assembly. Although this oscillator stabilises the initially unstable weave motion, it kills the self-stability of the bicycle; the steer-into-the-fall mechanism is made ineffective. The added pendulum mass is most noticeable in the diagonal mass matrix entry related to steering, $M_{\delta\delta}$, which increases from 0.25 to 0.46 kg m^2. More dramatic is the change in the constant symmetric stiffness matrix $g\mathbf{K}_0$, where the stiffness related to steering, $gK_{0\delta\delta}$, increases from a negative value, -6.6 N m/rad, to a positive value, 2.3 N m/rad, which partly explains the dramatic change in the eigenvalue structure.

4. Controllability

The controllability of the bicycles with passive rider models is investigated where either steer torque or upper body lean torque are considered as a control input. Therefore, both posture models will be extended with an extra degree of freedom to describe the upper body lean. The extended models for both postures are shown in Figure 6. The upper body lean angle θ is made possible by a hinge between the rear frame and the torso located at the saddle, position number 13 in Figure A1(b) of the appendix, with the hinge axis along the lengthwise x-direction.

The structure of the linearised equations of motion remains identical to that of Equation (1), but the number of equations increases from two to three. The three degrees of freedom for the lateral motion are now the rear frame roll angle, ϕ, the steer angle, δ, and the upper body lean angle, θ. The equations are linearised in the upright straight ahead configuration $(\phi, \delta, \theta) = (0, 0, 0)$ at a forward speed v and have the form of Equation (1) where the time-varying variables are now $\mathbf{q} = [\phi, \delta, \theta]^{\mathrm{T}}$ and the lean and steering torques are $\mathbf{f} = [T_\phi, T_\delta, T_\theta]^{\mathrm{T}}$.

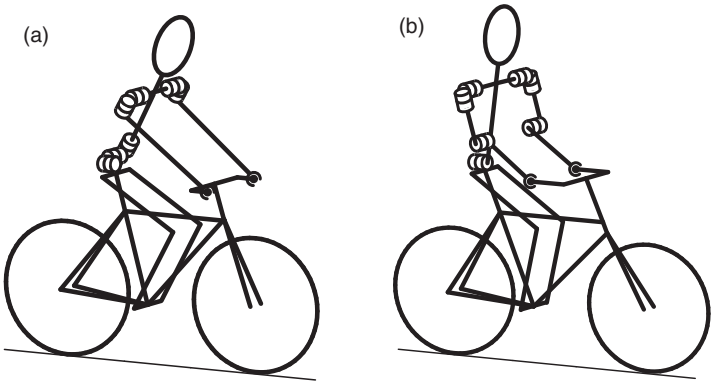

Figure 6. Two distinct bicycle models which include a leaned and steering rider: (a) rider with forward leaned body and stretched arms and (b) rider with upright body and flexed arms.

T_ϕ is an externally applied torque, and T_δ and T_θ are usually provided by a combination of internal torques in one or more of the joints of the arms and between the upper and lower body.

To investigate the controllability of the bicycle–rider system we rewrite these linearised equations of motion into a set of first-order differential equations, the so-called state–space equations, as

$$\dot{\mathbf{x}} = \mathbf{A}\mathbf{x} + \mathbf{B}\mathbf{u}, \tag{3}$$

with the state vector $\mathbf{x} = [\phi, \delta, \theta, \dot{\phi}, \dot{\delta}, \dot{\theta}]^{\mathrm{T}}$ and the control input vector $\mathbf{u} = [T_\delta, T_\theta]^{\mathrm{T}}$. The applied rear frame torque T_ϕ is not considered as a possible control input. Since we wish to address the control inputs separately, we split the input vector $\mathbf{u}$ and the associated matrix $\mathbf{B}$ into, respectively, two scalars and two associate vectors,

$$\dot{\mathbf{x}} = \mathbf{A}\mathbf{x} + \mathbf{b}_\delta T_\delta + \mathbf{b}_\theta T_\theta. \tag{4}$$

For the bicycle–rider system, the coefficient matrix, $\mathbf{A}$, and the control input vectors, $\mathbf{b}_\delta$ and $\mathbf{b}_\theta$, are given by

$$\mathbf{A} = \begin{bmatrix} \mathbf{0} & \mathbf{I} \\ -\mathbf{M}^{-1}(g\mathbf{K}_0 + v^2\mathbf{K}_2) & -\mathbf{M}^{-1}(v\mathbf{C}_1) \end{bmatrix}, \tag{5}$$

$$\mathbf{b}_\delta = \begin{bmatrix} \mathbf{0} \\ \mathbf{M}^{-1} \begin{bmatrix} 0 \\ 1 \\ 0 \end{bmatrix} \end{bmatrix}, \quad \mathbf{b}_\theta = \begin{bmatrix} \mathbf{0} \\ \mathbf{M}^{-1} \begin{bmatrix} 0 \\ 0 \\ 1 \end{bmatrix} \end{bmatrix}. \tag{6}$$

Note that the system of kinematic differential equations is controllable if $v \neq 0$ and $\cos\lambda_{\mathrm{s}} \neq 0$.

4.1. *Standard approach*

In the standard approach to determine controllability of a linear dynamical system as Equation (4), if the control input is restricted to a single variable, the controllability matrix

$$\mathbf{Q}_j = [\mathbf{b}_j, \mathbf{A}\mathbf{b}_j, \mathbf{A}^2\mathbf{b}_j, \ldots, \mathbf{A}^{k-1}\mathbf{b}_j], \tag{7}$$

is formed. If this controllability matrix has a full row rank k, where k is the dimension of the system, which is equal to the number of state variables, then the system is fully controllable by

Table 1. Forward speed v_u at which the hybrid bicycle with the forward leaned rider with stretched arms on the handlebar from Figure 6(a) is uncontrollable by either steer torque control T_δ or upper body lean torque control T_θ together with the corresponding eigenvalue λ_u and right eigenvector coordinates $(\phi, \delta, \theta)_u$, with rear frame lean angle ϕ, steer angle δ and upper body lean angle θ together with the mode description; see also Figure 7 for the eigenvalue plot.

v_u (m/s)	λ_u (rad/s)	$(\phi, \delta, \theta)_u$ (rad)	Mode
Steer torque control, T_δ			
0.0091	−3.0150	(0.14, 0.56, −0.82)	Capsize
1.5482	−3.0150	(0.15, 0.69, −0.71)	Capsize
1.7656	7.8250	(0.15, 0.71, −0.69)	Lean1
4.5588	−7.8250	(0.06, −0.28, 0.96)	Caster
Upper body lean torque control, T_θ			
0.0067	3.0177	(0.14, 0.56, −0.82)	Weave
1.5033	−3.0233	(0.15, 0.69, −0.71)	Capsize

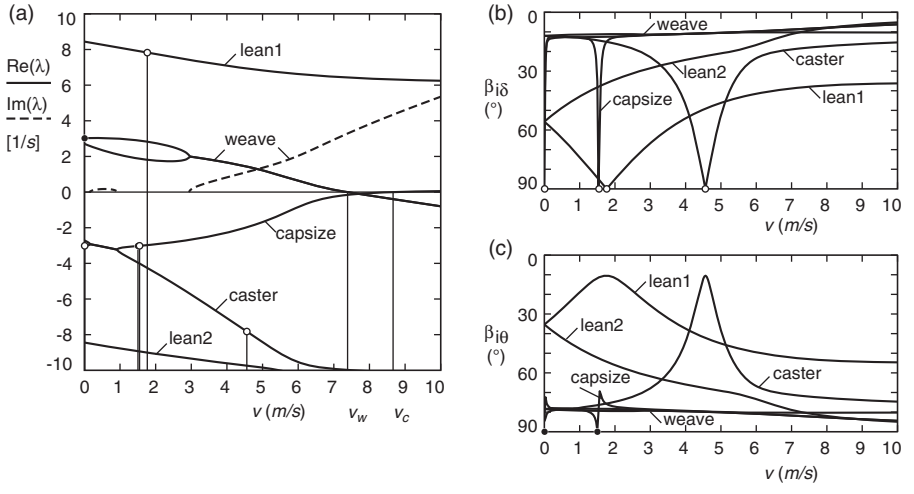

Figure 7. (a) Eigenvalues λ from the linearised stability analysis for the hybrid bicycle with the forward leaned rider with stretched arms on the handlebar from Figure 6(a), where the solid lines correspond to the real part of the eigenvalues and the dashed line corresponds to the imaginary part of the eigenvalues, in the forward speed range of $0\,\mathrm{m/s} < v < 10\,\mathrm{m/s}$, together with forward speeds for which the bicycle is uncontrollable by either steer torque (open circle) or upper body lean torque (black filled circle) alone. (b) Modal controllability $\beta_{i\delta}$ (8) for steer control torque T_δ for this bicycle model. (c) Modal controllability $\beta_{i\theta}$ (8) for an upper body control lean torque T_θ for this bicycle model.

input $j, j = \delta$ or $j = \theta$, alone. Here, we determine the speeds for which rank deficiency occurs by setting the determinant of $\mathbf{Q}_j(v)$ equal to zero and solving the resulting equation in v. The solutions are the forward speeds for which the system is uncontrollable with respect to the considered control input, which we call v_u. The corresponding eigenvector, $\mathbf{v}_u^*$, spans the null space of the transpose of the corresponding controllability matrix, $\mathbf{v}_u^* \in \mathrm{null}(\mathbf{Q}_j^T(v_u))$. Since this is also an eigenvector of the system matrix $\mathbf{A}^T(v_u)$, the corresponding eigenvalue λ_u can be found from the definition $\mathbf{A}^T\mathbf{v}_u^* = \lambda_u\mathbf{v}_u^*$. The corresponding right eigenvector $\mathbf{v}_u$ satisfies $\mathbf{A}\mathbf{v}_u = \lambda_u\mathbf{v}_u$ and gives the uncontrollable mode of the system. This procedure has been applied to the two bicycle–rider models and the results are presented in Table 1 and Figure 7 and in Table 2 and Figure 8.

For the hybrid bicycle with the forward leaned rider with stretched arms on the handlebar, controlled by steer torque control, we find four uncontrollable forward speeds, see Table 1

Table 2. As Table 1, but now for the city bicycle with an upright rider and flexed arms on the handlebar from Figure 6(b), see also Figure 8 for the eigenvalue plot.

v_u (m/s)	λ_u (rad/s)	$(\phi, \delta, \theta)_u$ (rad)	Mode
Steer torque control, T_δ			
0.0133	−2.8980	(0.16, 0.47, −0.87)	Caster
0.8271	6.5895	(0.14, 0.44, −0.89)	Lean1
1.0177	−2.8980	(0.14, 0.43, −0.89)	Caster
4.1381	−6.5895	(0.01, −0.26, 0.97)	Lean2
Upper body lean torque control, T_θ			
0.2695	2.9017	(0.16, 0.46, −0.87)	Capsize
1.2375	−2.9125	(0.13, 0.42, −0.90)	Caster

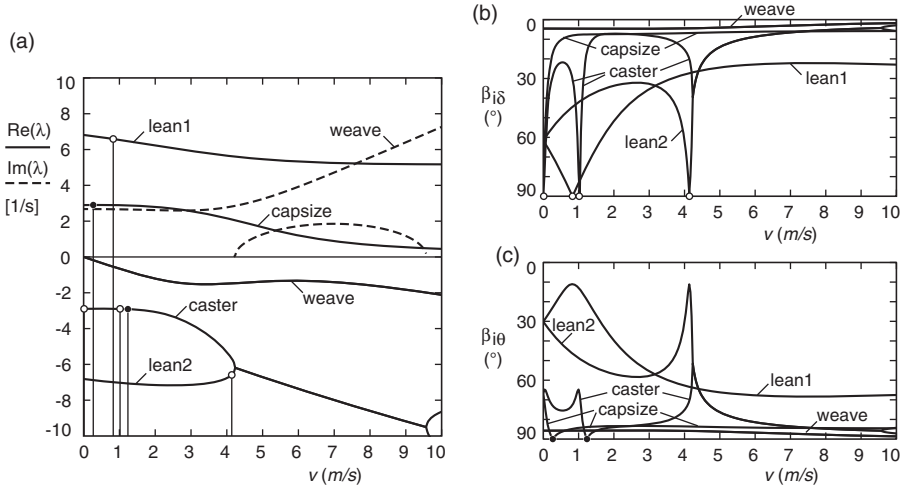

Figure 8. (a) Eigenvalues λ from the linearised stability analysis for the city bicycle with an upright rider and flexed arms on the handlebar from Figure 6(b), where the solid lines correspond to the real parts of the eigenvalues and the dashed line corresponds to the imaginary part of the eigenvalues, in the forward speed range of $0\,\mathrm{m/s} < v < 10\,\mathrm{m/s}$, together with forward speeds for which the bicycle is uncontrollable by either steer torque (open circle) or upper body lean torque (black filled circle) alone. (b) Modal controllability $\beta_{i\delta}$ (8) for steer control torque T_δ for this bicycle model. (c) Modal controllability $\beta_{i\theta}$ (8) for an upper body control lean torque T_θ for this bicycle model.

and Figure 7(a). However, only the one at 1.7656 m/s concerns an unstable mode, an upper body lean mode. This mode can be stabilised by placing a spring and a damper in parallel between the lower and upper body. For a spring stiffness of 100 N m/rad and a damping coefficient of 10 N m s/rad, the lean modes become stable and oscillatory, whereas the other modes change. The uncontrollability shifts to a much lower speed and corresponds to a weave mode. If we consider only upper body lean torque control, then there are two uncontrollable forward speeds, but again only one, now at 0.0067 m/s, concerns an unstable mode. This mode is the forerunner to the oscillatory weave mode, but since the speed is almost zero, this is again of no concern to the practical control of the bicycle. Adding a spring and damper acting in parallel with the control torque has no influence on the controllability. We conclude that this bicycle–rider configuration is fully controllable by either steer torque control or upper body lean torque control.

For the city bicycle with an upright rider and flexed arms on the handlebar we first find that the eigenvalue structure differs considerably from that of the hybrid bicycle with rider configuration. Whereas the hybrid bicycle had a stable forward speed range, between 7.4 and 8.7 m/s, the city bicycle configuration is always unstable. Although the weave mode is now

always stable, there is a capsize mode which is always unstable. For steer torque control on the city bicycle configuration (see Table 2 and Figure 8(a)), we find again four forward speeds for which the bicycle is uncontrollable, where only the one at 0.8271 m/s concerns an unstable mode. As with the hybrid bicycle, this is again an upper body lean mode that can be stabilised by adding a spring and a damper between the lower and the upper body; again, this shifts the uncontrollability to a much lower speed for the weave mode. For upper body lean control we have two uncontrollable speeds, where only the one at 0.2695 m/s concerns an unstable capsize mode. But since this is at a very low speed, one can say that, from a practical point of view, this configuration is also fully controllable by either steer torque control or upper body lean torque.

4.2. *Modal controllability*

The standard approach as described above results in a discrete set of velocities for which the bicycle is uncontrollable. It does not tell us anything about the ease or difficulty with which the bicycle is controlled in the neighbourhood of these speeds at which controllability is lost. To investigate that, we will follow a somewhat different approach and look at the modal controllability.

A measure for modal controllability has been proposed by Hamdan and Nayfeh [11]. They measure modal controllability by the angle β_{ij} between the left eigenvector $\mathbf{v}_i^*$ from $\mathbf{A}^{\mathrm{T}}\mathbf{v}_i^* = \lambda_i \mathbf{v}_i^*$, and the control input vector $\mathbf{b}_j$, as in

$$\cos\beta_{ij} = \frac{\mathbf{v}_i^{*\mathrm{T}}\mathbf{b}_j}{\|\mathbf{v}_i^*\|\|\mathbf{b}_j\|}. \tag{8}$$

They argue that, if the two vectors are orthogonal, then $\mathbf{v}_i^*$ is in the left null-space of $\mathbf{b}_j$ and the ith eigenmode is uncontrollable from the jth input. If the angle is not a right angle but nearly so, then again this indicates that the ith eigenmode is not easily controlled from the jth input. This modal controllability is applied to the two bicycle–rider models from Figure 6.

For steer torque control on the hybrid bicycle with the forward leaned rider with stretched arms on the handlebar, the modal controllability $\beta_{i\delta}$ is shown in Figure 7(b). Note that the vertical scale for the modal controllability angle β_{ij} runs from down 90° (uncontrollable) to up 0° (well controllable). Clearly, the unstable weave mode is well controllable. We also see two sharp dips in the capsize mode controllability near the uncontrollable speeds. It is interesting to see that the uncontrollability is so local, but since this capsize mode is still a stable mode, it is of no practical concern. What we call the caster mode shows a broad dip around the uncontrollable forward speed of 4.6 m/s, which seems paradoxical, because we use steer torque control, but note that there is still some steer amplitude in the corresponding eigenvector $(\phi, \delta, \theta)_{\mathrm{u}} = (0.06, -0.28, 0.96)$ (Table 1). As expected, the unstable upper body lean mode (lean1) is marginally controllable by steer torque control and shows a wide dip around the uncontrollable speed of 1.8 m/s. The modal controllability for upper body lean torque control on this bicycle–rider model is shown in Figure 7(c). Here, we see that the modal controllability of the unstable weave mode is close to 90° and therefore hard to control by lateral upper body motions. The same holds for the capsize mode, with a notable small rise of the modal controllability just above the speed for which the mode in uncontrollable. The caster mode also shows marginal controllability. The unstable upper body lean mode (lean1) is well controllable, which we would expect, but its modal controllability levels off at higher speeds. Note that the modal controllability for the lean torque input is almost the complement of the one for the steer torque input, meaning that the two inputs taken together make the system well controllable.

The modal controllability of the city bicycle with the upright rider and flexed arms on the handlebar for steer torque control is shown in Figure 8(b). The unstable capsize mode and the stable weave mode are well controllable. In the stable caster and lean2 modes, we see sharp dips around the uncontrollable speeds and here again the unstable upper body lean is marginally controllable by this steer torque control. The modal controllability for upper body lean torque control on this bicycle–rider model is shown in Figure 8(c). The same trends as in the hybrid bicycle are present, meaning that the unstable mode, here the capsize mode, is hard to control by upper body lean motions. It is interesting to see that the overall structure of the modal controllability is about the same as in the hybrid bicycle, although the structure of the eigenvalues with respect to forward speed is completely different.

We conclude that for both bicycle–rider combinations the controllability of the unstable modes is very good for steer torque control and marginal for upper body lean motions. The uncontrollable speeds, which are present, are of no real concern since they are either at stable modes which are not practically important for the overall desired motion or at very low forward speeds for which human control is difficult because of the relatively large positive real parts of the unstable eigenvalues.

5. Conclusions

Adding a passive upper body to the three degrees of freedom Whipple model of an uncontrolled bicycle, without adding any extra degrees of freedom, can change the open-loop dynamics of the system. In the case of a forward leaned rider with stretched arms and hands on the handlebar, there is little change. However, an upright rider position with flexed arms and hands on the handlebar changes the open-loop dynamics drastically and ruins the self-stability of the system.

The unstable modes of both bicycle–rider combinations have very good modal controllability for steer torque control but are marginally controllable by lateral upper body motions. This indicates that most control actions for lateral balance on a bicycle are performed by steer control only and not by lateral upper body motions.

Future work is directed towards the comparison of the control effort of the human rider in both postures.

Acknowledgement

Thanks to Jason Moore for measuring the bicycles and riders during his Fulbright granted year (2008/2009) at TU Delft and thanks to Batavus (Accell Group) for supplying the bicycles.

References

[1] K.J. Åström, R.E. Klein, and A. Lennartsson, *Bicycle dynamics and control*, IEEE Control Syst. Mag. 25(4) (2005), pp. 26–47.
[2] J.P. Meijaard, J.M. Papadopoulos, A. Ruina, and A.L. Schwab, *Linearized dynamics equations for the balance and steer of a bicycle: a benchmark and review*, Proc. Roy. Soc. A 463 (2007), pp. 1955–1982.
[3] R.S. Sharp, *On the stability and control of the bicycle*, Appl. Mech. Rev. 61 (2008), pp. 060803-1–24.
[4] F.J.W. Whipple, *The stability of the motion of a bicycle*, Quart. J. Pure Appl. Math. 30 (1899), pp. 312–348.
[5] J.D.G. Kooijman, J. Moore, and A.L. Schwab, *Some observations on human control of a bicycle*, in *11th mini Conference on Vehicle System Dynamics, Identification and Anomalies (VSDIA2008), Budapest, Hungary*, I. Zobory, ed., Budapest University of Technology and Economics, 2008, pp. 65–72.
[6] J.K. Moore, J.D.G. Kooijman, and A.L. Schwab, *Rider motion identification during normal bicycling by means of principal component analysis*. in *MULTIBODY DYNAMICS 2009, ECCOMAS Thematic Conference, 29 June–2 July 2009*, K. Arczewski, J. Frączek and M. Wojtyra, eds., Warsaw, Poland, 2009.

[7] M. Nagai, *Analysis of rider and single-track-vehicle system; its application to computer-controlled bicycles*, Automatica 19(6) (1983), pp. 737–740.
[8] K.A. Seffen, G.T. Parks, and P.J. Clarkson, *Observations on the controllability of motion of two-wheelers*, Proc. Inst. Mech. Eng. I J. Syst. Control Eng. 215(2) (2001) pp. 143–156.
[9] R.S. Sharp, *The stability and control of motorcycles*, J. Mech. Eng. Sci. 13(5) (1971), pp. 316–329.
[10] B. Friedland, *Controllability index based on conditioning number*, J. Dyn. Syst. Meas. Control 97(4) (1975), pp. 444–445.
[11] A.M.A. Hamdan and A.H. Nayfeh, *Measures of modal controllability and observability for first- and second-order linear systems*, J. Guidance Control Dyn. 12(3) (1989), pp. 421–428.
[12] J.D.G. Kooijman, A.L. Schwab, and J.P. Meijaard, *Experimental validation of a model of an uncontrolled bicycle*, Multibody Syst. Dyn. 19 (2008), pp. 115–132.
[13] J.K. Moore, M. Hubbard, J.D.G. Kooijman, and A.L. Schwab, *A method for estimating physical properties of a combined bicycle and rider*, Proceedings of the ASME 2009 International Design Engineering Technical Conferences & Computers and Information in Engineering Conference, DETC2009, 30 August–2 September, San Diego, CA, 2009.
[14] J.B. Jonker and J.P. Meijaard, *SPACAR - Computer program for dynamic analysis of flexible spatial mechanisms and manipulators*, in *Multibody Systems Handbook*, W. Schiehlen, ed., Springer, Berlin, Germany, 1990, pp. 123–143.
[15] A.L. Schwab and J.P. Meijaard, *Dynamics of flexible multibody systems having rolling contact: Application of the wheel element to the dynamics of road vehicles*. Veh. Syst. Dyn. (Suppl.) 33 (2000), pp. 338–349.
[16] A.L. Schwab and J.P. Meijaard, *Dynamics of flexible multibody systems with non-holonomic constraints: A finite element approach*, Multibody Syst. Dyn. 10(1) (2003), pp. 107–123.

Appendix 1. Measured bicycle and rider data

This appendix summarises the measured geometric and mass data of the bicycles and rider used, measured according to [13]. The first bicycle, Figure 1(a), can be characterised as a hybrid bicycle. The second bicycle, Figure 1(b), is a standard Dutch city bicycle (see Figure A1).

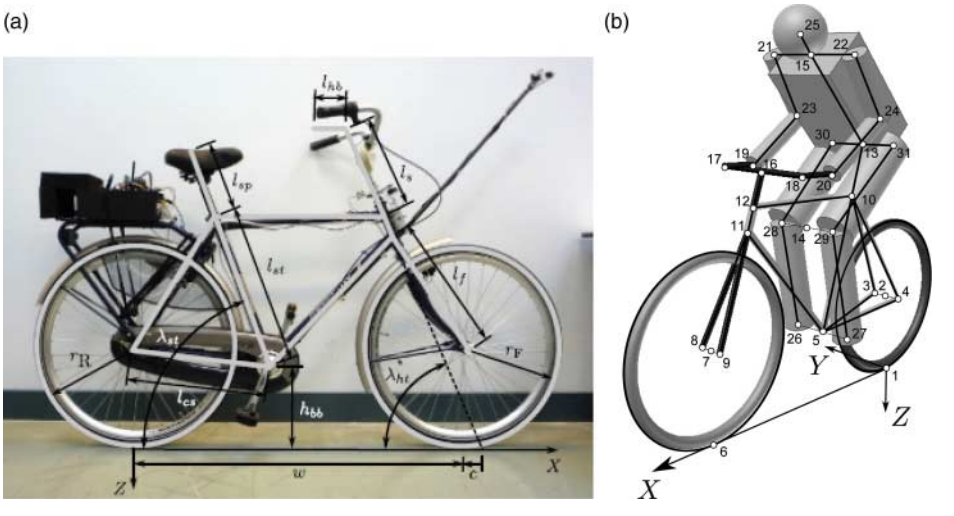

Figure A1. (a) Definition of the geometric parameters of the bicycle and (b) rider model with skeleton points, from [13].

Table A1. Bicycle geometric dimensions for the hybrid bicycle and the city bicycle according to Figure A1(a).

Parameter	Symbol	Value for hybrid bicycle	Value for city bicycle
Bottom bracket height	h_{bb}	0.290 m	0.295 m
Chain stay length	l_{cs}	0.445 m	0.460 m
Fork length	l_f	0.455 m	0.455 m
Front hub width	w_{fh}	0.100 m	0.100 m
Handlebar length	l_{hb}	−0.090 m	0.190 m
Rear hub width	w_{rh}	0.130 m	0.130 m
Seat post length	l_{sp}	0.195 m	0.240 m
Seat tube angle	λ_{st}	75.0°	68.5°
Seat tube length	l_{st}	0.480 m	0.530 m
Stem length	l_s	0.190 m	0.250 m
Wheel base	w	See Table A2	
Trail	c	See Table A2	
Head tube angle	$\lambda_{ht} = 90° - \lambda_s$	See Table A2	
Rear wheel radius	r_R	See Table A2	
Front wheel radius	r_F	See Table A2	

Table A2. Parameters for the hybrid bicycle and the city bicycle for the bicycle model from Figure 2.

Parameter	Symbol	Value for Hybrid Bicycle	Value for City Bicycle
Wheel base	w	1.037 m	1.121 m
Trail	c	0.0563 m	0.0686 m
Steer axis tilt	λ_s	16.9°	22.9°
Gravity	g	9.81 N/kg	9.81 N/kg
Forward speed	v	*various* m/s	*various* m/s
Rear wheel R			
Radius	r_R	0.338 m	0.341 m
Mass	m_R	3.96 kg	3.11 kg
Inertia	(I_{Rxx}, I_{Ryy})	(0.0916, 0.1545) kg m^2	(0.0884, 0.1525) kg m^2
Rear Body and frame assembly B			
Centre of mass	(x_B, z_B)	(0.3263, −0.4826) m	(0.2760, −0.5378) m
Mass	m_B	7.22 kg	9.86 kg
Inertia	$\begin{bmatrix} I_{Bxx} & 0 & I_{Bxz} \\ 0 & I_{Byy} & 0 \\ I_{Bxz} & 0 & I_{Bzz} \end{bmatrix}$	$\begin{bmatrix} 0.37287 & 0 & 0.03835 \\ 0 & 0.71704 & 0 \\ 0.03835 & 0 & 0.45473 \end{bmatrix}$ kg m^2	$\begin{bmatrix} 0.52714 & 0 & 0.11442 \\ 0 & 1.31682 & 0 \\ 0.11442 & 0 & 0.75920 \end{bmatrix}$ kg m^2
Front Handlebar and fork assembly H			
Centre of mass	(x_H, z_H)	(0.9107, −0.7303) m	(0.8669, −0.7482) m
Mass	m_H	3.04 kg	3.22 kg
Inertia	$\begin{bmatrix} I_{Hxx} & 0 & I_{Hxz} \\ 0 & I_{Hyy} & 0 \\ I_{Hxz} & 0 & I_{Hzz} \end{bmatrix}$	$\begin{bmatrix} 0.17684 & 0 & 0.02734 \\ 0 & 0.14437 & 0 \\ 0.02734 & 0 & 0.04464 \end{bmatrix}$ kg m^2	$\begin{bmatrix} 0.25338 & 0 & -0.07205 \\ 0 & 0.24610 & 0 \\ -0.07205 & 0 & 0.09558 \end{bmatrix}$ kg m^2
Front wheel F			
Radius	r_F	0.340 m	0.344 m
Mass	m_F	3.334 kg	2.02 kg
Inertia	(I_{Rxx}, I_{Ryy})	(0.09387, 0.15686) kg m^2	(0.09041, 0.14939) kg m^2

Table A3. Anthropomorphic data for Rider A according to Figure A1(b).

Parameter	Symbol	Rider A
Chest circumference	c_{ch}	0.94 m
Forward lean angle	λ_{fl}	63.9° (on hybrid bicycle) 82.9° (on city bicycle)
Head circumference	c_h	0.58 m
Hip joint to hip joint	l_{hh}	0.26 m
Lower arm circumference	c_{la}	0.23 m
Lower arm length	l_{la}	0.33 m
Lower leg circumference	c_{ll}	0.38 m
Lower leg length	l_{ll}	0.46 m
Shoulder to shoulder	l_{ss}	0.44 m
Torso length	l_{to}	0.48 m
Upper arm circumference	c_{ua}	0.30 m
Upper arm length	l_{ua}	0.28 m
Upper leg circumference	c_{ul}	0.50 m
Upper leg length	l_{ul}	0.46 m
Rider mass	m_{Br}	72.0 kg
Head mass	m_h	0.068 m_{Br}
Lower arm mass	m_{la}	0.022 m_{Br}
Lower leg mass	m_{ll}	0.061 m_{Br}
Torso mass	m_{to}	0.510 m_{Br}
Upper arm mass	m_{ua}	0.028 m_{Br}
Upper leg mass	m_{ul}	0.100 m_{Br}

Table A4. Skeleton points code according to Figure A1.

```
%% Matlab code for Skeleton Grid Points see Figure A1a
%% Adapted Table 10 from MooreHubbardKooijmanSchwab2009
r1 = [0 0 0];
r2 = [0 0 -rR];
r3 = r2 + [0 wrh/2 0];
r4 = r2 + [0 -wrh/2 0];
r5 = [sqrt(lcs^2-(rR-hbb)^2) 0 -hbb];
r6 = [w 0 0];
r7 = r6 + [0 0 -rF];
r8 = r7 + [0 wfh/2 0];
r9 = r7 + [0 -wfh/2 0];
r10 = r5 + [-lst*cos(last) 0 -lst*sin(last)];
% calculate f0
f0 = rF*cos(laht)-c*sin(laht);
r11 = r7 + [-f0*sin(laht)-sqrt(lf^2-f0^2)*cos(laht)…
  0 f0*cos(laht)-sqrt(lf^2-f0^2)*sin(laht)];
r12 = [r11(1)-(r11(3)-r10(3))/tan(laht) 0 r10(3)];
r13 = r10 + [-lsp*cos(last) 0 -lsp*sin(last)];
% determine mid knee angle and mid knee position
a1 = atan2((r5(1)-r13(1)),(r5(3)-r13(3)));
l1 = sqrt((r5(1)-r13(1))^2+(r5(3)-r13(3))^2);
a2 = acos((l1^2+lul^2-lll^2)/(2*l1*lul));
%
r14 = r13 + [lul*sin(a1+a2) 0 lul*cos(a1+a2)];
r15 = r13 + [lto*cos(lafl) 0 -lto*sin(lafl)];
r16 = r12 + [-ls*cos(laht) 0 -ls*sin(laht)];
r17 = r16 + [0 lss/2 0];
r18 = r16 + [0 -lss/2 0];
r19 = r17 + [-lhb 0 0];
r20 = r18 + [-lhb 0 0];
r21 = r15 + [0 lss/2 0];
r22 = r15 + [0 -lss/2 0];
% determine left elbow position
a1 = atan2((r19(1)-r21(1)),(r19(3)-r21(3)));
```

Table A4. Continued

```
l1 = sqrt((r19(1)-r21(1))^2+(r19(3)-r21(3))^2);
a2 = acos((l1^2+lua^2-lla^2)/(2*l1*lua));
%
r23 = r21 + [lua*sin(a1-a2) 0 lua*cos(a1-a2)];
r24 = r23 + [0 -lss 0];
r25 = r15 + [ch/(2*pi)*cos(lafl) 0 -ch/(2*pi)*sin(lafl)];
r26 = r5 + [0 lhh/2 0];
r27 = r5 + [0 -lhh/2 0];
r28 = r14 + [0 lhh/2 0];
r29 = r14 + [0 -lhh/2 0];
r30 = r13 + [0 lhh/2 0];
r31 = r13 + [0 -lhh/2 0];
```